Molecular dynamics study of the mechanism of ion transport in lithium silicate glasses: Characteristics of the potential energy surface and structures

Junko Habasaki*
Tokyo Institute of Technology, 4259 Nagatsuta-cho, Yokohama, Kanagawa, 226-8502, Japan

Yasuaki Hiwatari
Kanazawa University, Kakuma, Kanazawa 920-1192, Japan

(Received 7 July 2003; revised manuscript received 10 October 2003; published 16 April 2004)

Characterization of the potential energy surface is one of the essential problems to understand the mechanism of the ion conduction in glasses. In this work, ion dynamics in several lithium silicate glasses are examined by using molecular dynamics simulations. The number of ion sites, site energy, and the respective structures were examined for both fast (diffusive) and slow (localized) ions. We have visualized ion sites using the molecular dynamics simulation data and obtained the number of sites without being affected by a cut off value. The number obtained for the Li_2SiO_3 glass is 8–10% larger than that of ions. The value is reasonable to explain the diffusion mechanism by cooperative jumps, since rapid decrease of transport property in cooperative dynamics is expected if the number of the sites is too small while the cooperative jumps may be scarcely observed when the number of the vacancy is too large. The percentage of the available sites for the Li_4SiO_4 in the glassy state was found to be almost the same as that for Li_2SiO_3, while the diffusion coefficient of Li in Li_4SiO_4 is larger than Li_2SiO_3. Increase of the diffusion coefficient with increasing alkali contents is easily explained by the contribution of the cooperative jumps but not by a simple mobile vacancy mechanism. Besides the characteristic sites for each slow (type A) and fast (type B) ions, many common sites for both type of ions are found, while the steepest descent energy distribution for these types of ions is quite similar. On the other hand, the partial pair correlation function, $g(r)$ of A-A pairs is found to be quite different from that of B-B pairs. Therefore, microstructures related to the density fluctuation of the Li ions are important for the difference of slow and fast dynamics.

DOI: 10.1103/PhysRevB.69.144207 PACS number(s): 61.20.−p, 63.50.+x, 05.10.−a

I. INTRODUCTION

The mechanism of ion migration in ion conducting glasses has been examined by several techniques. Molecular dynamics simulation (MD) is one of the useful tools to understand the microscopic origin of the dynamics. In previous MD works, we have characterized the ion dynamics by jump motions and observed both fast dynamics by cooperative jumps and the slow dynamics due to localized jumps (fracton) and long waiting time of jump motions in lithium silicate glasses.[1–3] Recently, Cormack *et al.*[4] have investigated the ion dynamics in sodium silicate glasses by MD and have observed a few sequences of jumps between selected sites. They interpreted the resulting dynamics as the motion of vacancies and suggested that the identification of all sites in the glass would be useful for a deeper understanding of the mechanism. Thus the number of the available sites is one of the fundamental problems to distinguish the possible mechanism of the ion migration. Lammert *et al.*[5] counted the number of available sites in lithium silicate glasses, $(Li_2O)_x(SiO_2)_{1-x}$ ($x=0.5$ and $x=0.1$), using MD simulation with potential parameters obtained by us. They divided the simulation box into cubic cells with size $\approx (0.3\ \text{Å})^3$ and counted during MD run how many time steps a cell is visited by a lithium ion. To identify the ionic sites and to eliminate the paths between the sites, cells with only a few counts are dismissed. Their method is simple and useful for characterization of the dynamics, if the ionic sites and the paths between the sites are correctly separated.

They found that the available sites for lithium metasilicate were 3% larger than the number of lithium ions and mentioned that the theoretical description of the dynamics in terms of the mobile vacancies is most appropriate. As discussed in the Ref. 3, effective jump path formed by the fast ions has low dimensionality, where several ions move almost at the same time. If ions are completely surrounded by vacancies, ion cannot move cooperative manner with other Li ions. This means that the conduction path is formed in a dense part of the Li ions and the number of available site should be small to form the effective jump path. Qualitatively, their results are consistent to ours and it is unsurprising that the space for lithium ion is fairly limited in the glassy state. In the present work, the number of ion sites in several lithium silicate glasses was also examined for clarifying the following problem. By using Monte Carlo simulations for a simplified case with and without block particles in Lennard-Jones system,[6] it was demonstrated that diffusion coefficient in a high-density region decreases with decreasing number of empty sites and the limit value is 0. Naturally, we can expect that the rapid decrease of diffusion coefficient with decreasing number of available sites near the high-density limit and that this trend is emphasized when the cooperative jumps exist[6] due to the sensitivity of the cooperative jumps to the blockage. Such situation is clearly observed in the mixed alkali system. In the previous MD studies,[7–10] we have shown that the ''mixed alkali effect''[11–14] is caused

by the blockage by the foreign alkali ions where the suppression of the cooperative jumps plays an important role. Lammert *et al.* found that the number of available sites for the system with $x=0.1$ is larger than the system with $x=0.5$. In the system with larger alkali content, the number of empty sites may be smaller than 3%. However, lithium orthosilicate (Li_4SiO_4) ($x=0.67$) and its solid solution derivative systems, are known as an important class of fast Li-ion conducting materials. For example, see Ref. 15. How can we explain the high dc conductivity of the higher alkali content glass, if the possible path is almost blocked by like ions? Thus quantitative estimation of the number of the sites including ones dismissed by them is desirable to discuss the mechanism of the diffusion. We have divided the simulation box into cubic cells and counted during MD run how many time steps a cell is visited by a lithium ion. Then we looked for the cell having peak count instead of the cluster analysis by them. This procedure enables us to pick up every site without affected by the cutoff level. We also visualized the dynamical ion sites by a contour map. The method was also applied for the slow (type A) and fast (type B) Li ions defined as follows in Li_2SiO_3 at 700 K. The particles showing a squared displacement less than squared distance equal to the first minimum of the Li-Li pair correlation function $g(r)$ is defined as type A, namely, the ion is located within neighboring sites during a given time, $T(=920$ ps). While ions showing squared displacements greater than squared distance equal to the first minimum of $g(r)$ within this time scale are defined as type B, which can contribute to the long-time dynamics. This time scale is chosen because it is shorter than the time scale of exchanges between slow and fast dynamics and longer than t_{x2} (where the separation of the slow and fast dynamics becomes clearer as explained in our previous paper[16]), so that the difference of fast and slow dynamics can be observed clearly. Steepest descent method[17] has been applied for both types of ions to examine the relation between potential energy of the site and the dynamics. We cannot find remarkable differences between type A and B in the site energies. On the other hand, difference in the structure of intermediate length scale has been found when we examine the pair correlation function $g(r)$ of Li-Li with distinguishing type A and B ions. Relationships between the characteristics of the potential surface and dynamics will be discussed.

II. MOLECULAR DYNAMICS SIMULATIONS

MD simulations and analysis in these works were performed using our programs. The numbers of the particles in the basic cube were 144 Li, 72 Si, and 216 O for Li_2SiO_3, while the numbers are 192 Li, 48 Si and 192 O for Li_4SiO_4. Larger systems containing total 3456 particles were used for several cases of above systems and for $Li_2Si_3O_7$ (576 Li, 864 Si, and 2016 O). For the former fragile systems, the larger system is not necessarily required[1,10] to obtain proper dynamics. The results of the analysis for the smaller systems will be shown unless otherwise stated. On the other hand, for $Li_2Si_3O_7$, the larger system is necessary due to stronger coupling with the higher-dimensional framework structures compared with Li_2SiO_3. The volume was fixed as that derived by NPT (constant pressure and temperature) ensemble simulation. Computer glass transition temperatures of the simulated systems determined by the plot of volume against temperature relations were approximately 830 K for the lithium metasilicate. Pair potential functions of Gilbert-Ida type[18] with r^{-6} terms were used. The parameters of the potentials used were previously derived on the basis of *ab initio* molecular orbital calculations,[19] and their validity was checked in the liquid, glassy, and crystal states under constant pressure conditions. Several MD runs, 2–10 ns (500 000–2500 000 steps), were performed for each system at several temperatures in the glassy and supercooled liquid states (600 K, 700 K, 800 K, and 1000 K). Using a sequence of particle positions during a run of T_1 period, we prepared N arrays of data sequence with slightly shifted t_0 values and the data for N arrays were averaged. Then the time window δW is a time range covered by chosen t_0 values. A larger time window than 400 ps and N values larger than 400 were used to obtain the diffusion coefficients. Positions of ions were checked every 0.8 ps during about 1 ns run and the number of jumps for each ion was counted in the several conditions. Displacement greater than 1/2 of the distance of the first maximum of the pair correlation function of Li-Li was taken as a jump. The number of jumps thus defined is correlated well with those among jump sites observed in this work, but includes jump trials. Characteristics of the ion sites were examined for these systems in the glassy state. The method to obtain the number of sites will be described later in detail. Steepest descent method[17] was applied for Li_2SiO_3 (for a larger system) at $t=0$ as similar manner in our previous work.[7] A part of the MD runs in the larger systems has been performed by using accelerator boards (Fuji Xerox MD Engine II).

III. RESULTS AND DISCUSSIONS

A. Heterogeneity of the dynamics of lithium ions

As shown in our previous works, ion dynamics is extremely heterogeneous.[1–3,20] Characteristics of fast and slow dynamics are summarized here, because this is fundamental to understand the relation of dynamics and the multidimensional potential surfaces discussed in this paper. With cooperative jumps (neighboring ions jump almost at the same time to almost the same direction), fast ions can go further than neighboring sites and thereby contribute to the long-time diffusive dynamics. This kind of motion has strong forward correlation probability because if the jump followed by a jump of another particle to the original site immediately, no backward motion is possible. The dynamics has been characterized as the Lévy flight dynamics[21,22] where the cooperation play a role to cause large forward correlation probability of the ions, which resulted in the acceleration of the dynamics. Without this type of motion, ion cannot diffuse long distance since high density of the glassy material cause a strong back correlation probability of the ionic motion, that is, ion performing a single jump has strong tendency of returning to its original site since other destinations of the ion tend to be occupied. This kind of behavior can be explained as ''fracton''[23] of jump version, related with low-dimensional

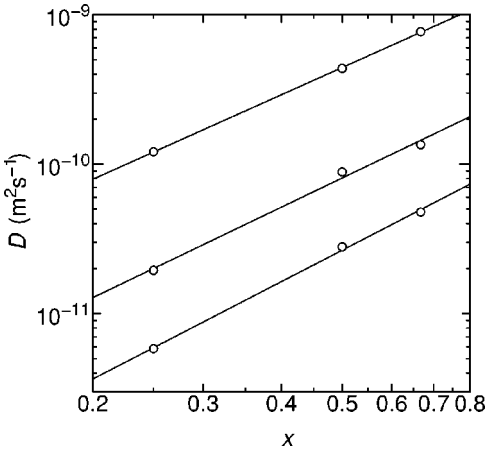

FIG. 1. Diffusion coefficient isotherms at 700 K, 800 K, and 1000 K of $(Li_2O)_x$-$(SiO_2)_{1-x}$ glasses.

local paths and large fractal dimension of random walks. Ions with long waiting time also contribute to the slow dynamics. Thus slow dynamics relevant for type A ions are due to long waiting time of jumps and localized jumps between neighboring sites (fractons), while the fast dynamics relevant for type B ions are accelerated dynamics due to cooperative jumps where the strong forward correlation resulted in long effective jump distances.

Definition of type A and B depends on the choice of T and δW due to the mixing of slow and fast dynamics in a longer time scale; nevertheless slow and fast dynamics in a certain time regime have distinct characters.[2] Since the main contribution of MSD in a longer time scale is due to type B ions with large forward correlation probability, the main mechanism of the ion transport is not single jumps but is cooperative jumps.

B. Isotherms of the diffusion coefficient in lithium silicate glasses

Mean-squared displacements of Li ions in lithium silicate systems were calculated from the MD data and diffusion coefficients were obtained from the slope in long time regions. Diffusion regime at 700 K is attained at about 700 ps, 300 ps, and 100 ps for $Li_2Si_3O_7$, Li_2SiO_3, and Li_4SiO_4 systems, respectively. Isotherms of the diffusion coefficients for the different alkali content glasses are shown in Fig. 1. An increase is observed even in the region $x>0.5$, and increase of the diffusion coefficients with the alkali content can be well represented by the power laws. DC conductivity tends to increase logarithmically with increase of alkali contents at least in the small alkali content region. Maass *et al.*[24] have explained the logarithmic composition dependence by the percolative aspect of the jump sites. We would like to point out that percolation of the conduction path is important to understand such behavior. Figure 2(b) shows the plot of squared displacement of each lithium ions against number of jumps of Li_4SiO_4 at 700 K. For the sake of the comparison, similar plot for Li_2SiO_3 is also shown in Fig. 2(a). The squared distance corresponds to the first minimum of $g(r)$ Li-Li is shown by a line in each figure. The points below this

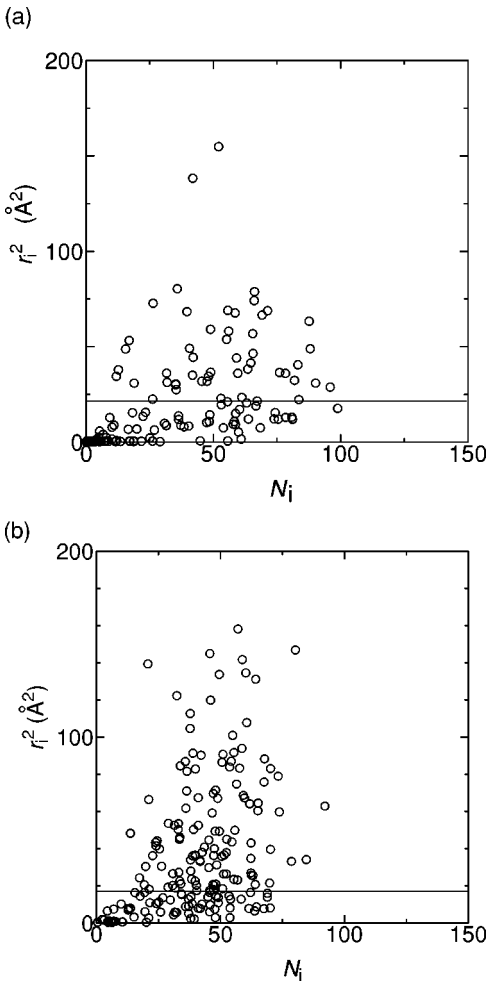

FIG. 2. Displacement against number of jumps for (a) Li_2SiO_3 and (b) Li_4SiO_4 system at 700 K during 920 ps. With increase of Li content, the number's ratio of type B and A ions increases.

line are for type A ions and those above the line are for type B ions. Definition of type A and B has some arbitrariness due to exchanges between slow and fast dynamics. We chose to compare the results based on the same T, since the difference in the total number of jumps per ion during T for Li_2SiO_3 and that in the Li_4SiO_4 is not so large, namely, the mean jump rate $\langle N_i \rangle / T$ is not sensitive to compositions. Using Fig. 2, we can compare the results of different compositions easily since the values for horizontal axis in Fig. 2 corresponds to the jump rate. The points near $N_i=0$, which corresponds to the long waiting time, are still found for Li_4SiO_4 but the number is smaller than those for the Li_2SiO_3. Both the number of type B ions and the ratio of type B ions to type A ions for Li_4SiO_4 is larger than that in Li_2SiO_3. As well as the increased contribution of type B ions with alkali content, the component with larger r_i^2/N_i values are frequently observed in Li_4SiO_4, that is, the displacement of type B ion per jump (effective jump length) in Li_4SiO_4 is longer than that in Li_2SiO_3 due to the strong forward correlation of the cooperative jumps. Even at $x=0.67$, the system still should have enough space to allow the cooperative jumps and this is fundamental to design the high-conductivity materials. On the

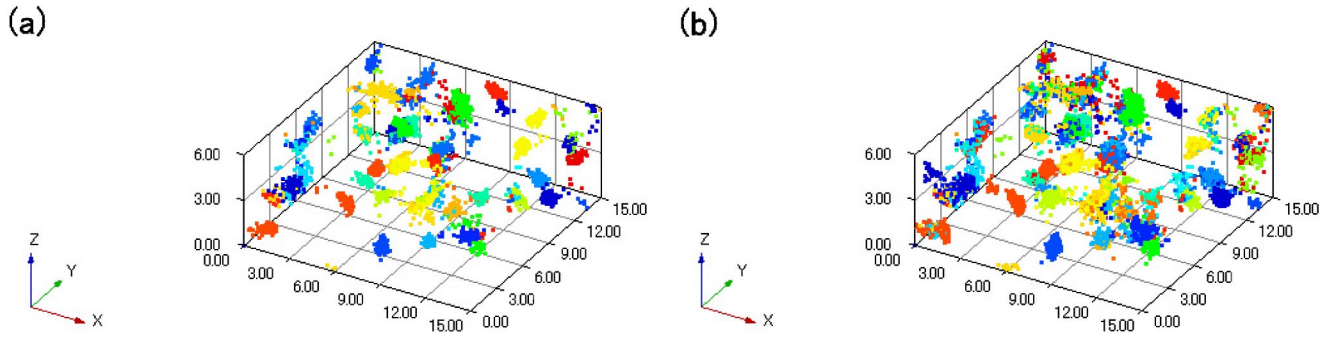

FIG. 3. (Color online) Positions (in angstrom) of Li ions during (a) 400 ps and (b) 1 ns at 700 K in Li_2SiO_3 plotted every 0.8 ps. Each Li ion has its own color.

other hand, distribution of N_i/T (jump rate) does not show large dependence on the alkali content. From this result, it is clear that main reason of the increase of diffusion coefficients with increasing alkali content is not by the changes in the jump rates (temporal term) but the increase of the effective jump distance per jump (spatial term) due to forward correlated jumps.

Thus in the dynamics of mobile ions in the glasses, the role of cooperative jumps in type B ions, which form the effective jump paths for the diffusion is quite important, and the concept of the percolation of the jump paths is required.

C. Analysis of the ion sites

Figure 3(a), and 3(b) shows the positions of lithium ions recorded every 0.8 ps during 400 ps and 1 ns at 700 K for Li_2SiO_3, for a part of the unit cell, respectively. The system contains 144 Li ions and each lithium ion has its own color in these figures. The number of points reflects the probability density of the ions during the run and corresponds the sum of the residence times for each site. Mixing of the colors and connection of the sites mean the formation of the jump path where many ions taking part in. Similar plots were used to determine the fractal dimension of the jump paths.[7,25] In Fig. 3(b), several new sites, which are not found in Fig. 3(a), may be found. However, it is fairly difficult to distinguish the sites and paths by the counts because of large overlap of them. Counts for some paths are larger than those for new sites found in the longer time region because of wide waiting time distribution of the jumps. In this situation, using cutoff value may cause large errors. To avoid this difficulty, we use the following methods to count the number of ion sites.

We divided the unit simulation box into cubic cells with $(L/20)^3$, where the L means the edge length of the basic cell of the simulation, and counted how many times a cell is visited by Li ions during a MD run. Using distribution of these counts, several contour maps were prepared. In Figs. 4(a) and 4(b), a contour map for an arbitrary chosen slice of L/20 in Li_2SiO_3 at 700 K is shown, where the counts during 4 ns were accumulated. We can easily distinguish the paths and sites by the maps.

Ion sites show clear peak counts and typical distance between the neighboring peaks naturally corresponds to the first peak of the $g(r)_{max}$(about 3 Å) of the Li-Li pairs in the glasses at low temperatures. Several ion sites are found to have anisotropy. The ion sites visualized by this way does not reflect the instantaneous potential well but include the decay of the cage in the near constant loss (NCL) regime,[16]

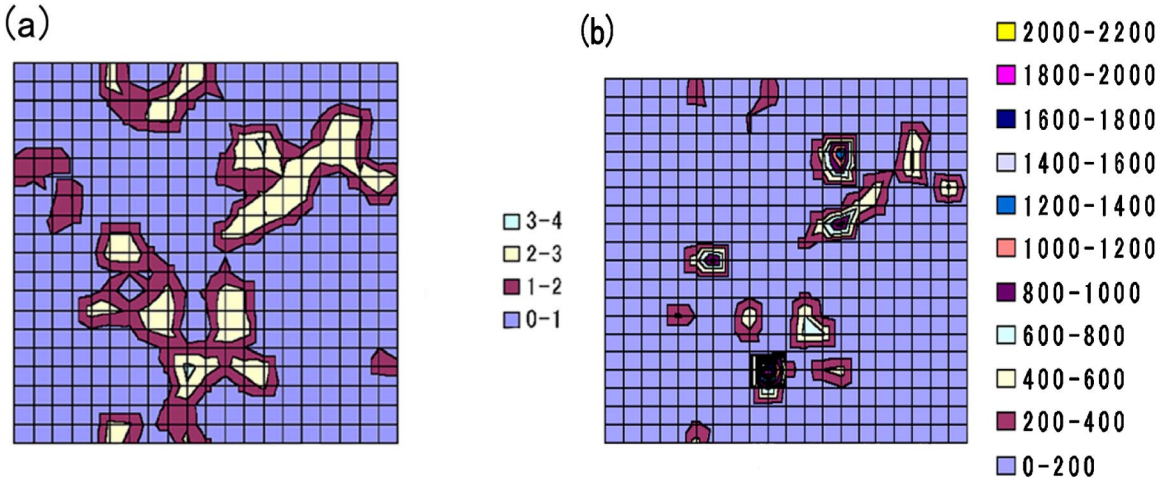

FIG. 4. (Color online) Jump sites visited by Li ions during 4 ns run for Li_2SiO_3 at 700 K are visualized by a contour map for a slice of the simulation box. Contours are shown (a) on a log scale and (b) on a linear scale. The expression in the legend in (a), such as 1-2 means the values from 10^1 to 10^2.

TABLE I. Number of ion sites. The values in the parentheses are excess amount of the ion sites (percent) compared with the number of alkali metal ions.

T	System					
	$Li_2Si_3O_7$					
700 K	Run I [a]					
	1 ns	648(12.5)				
	2 ns	666(15.6)				
	4 ns	688(19.2)				
800 K	Run I		Run II [a]			
			400 ps	634(10.1)		
	1 ns	84(16.7)	1 ns	686(19.1)		
	2 ns	99(37.5)				
	4 ns	100(38.9)				
	6 ns	107(48.6)				
	Li_2SiO_3					
600 K	Run I					
	1 ns	155(7.6)				
	5 ns	156(8.3)				
	10 ns	156(8.3)				
700 K	Run I		Run II		Run III [a]	
	1 ns	155(7.6)	1 ns	159(10.4)		
			2 ns	159(10.4)	2 ns	1244(8.0)
			4 ns	159(10.4)		
	5 ns	157(9.0)				
	10 ns	157(9.0)				
800 K	Run I		Run II			
	1 ns	161(11.8)	1 ns	161(11.8)		
			2 ns	158(9.7)		
			4 ns	171(18.8)		
	Li_4SiO_4					
700 K	Run I					
	1 ns	210(9.4)				
	2 ns	210(9.4)				

[a]The system contains 3456 particles in the basic simulation box. Other systems consist of 432 particles.

that is, anisotropy is caused by the motion of cage in the NCL regime. The number of cells (20^3) is large enough to distinguish each site clearly, although larger number of cells may be required if one desires to analyze the details of the jump sites such as the shape and/or anisotropy. In Fig. 4(a), heights of the contours are shown on a log scale, while in Fig. 4(b), those are shown on a linear scale. The probability density of the counts changes over several orders due to the wide distribution of the waiting times of the jumps and the counts for paths connecting jump sites are sometimes greater than that for the ion sites.

Two methods are used to count the number of sites here. One is direct counting by eyes using contour maps of the all slices of the basic simulation box. Another is looking for the cell with peak count by the program, in which counts in neighboring cells (with face sharing, edge sharing and corner sharing) are compared and the peak positions and counts are recorded. Separation of the peaks and the path is well established since the distribution of the peak counts does not show any contribution of the path. Direct counting by eyes is not so easy when the site is near the edge or the corner of the slice. On the other hand, in counting by the program, convergence of two groups of counts on one was found in a longer time run. We decided to use the values obtained by the program for further discussion, since results of these methods are coincident each other within ± 2 sites in several cases. Only undeveloped sites less than 5 counts at the peak, which correspond to 0.1% of the highest peak for the 4 ns run, are dismissed in the program. The number of sites thus obtained and the excess percentage of it compared with the number of ions are shown in Table I. The results obtained by the run with larger system size are also shown in this table. In these cases, $L/40$ was used as a size of the cell. For Li_2SiO_3 and Li_4SiO_4, the number of sites seems to be slightly increasing with elapse of time and increasing temperature. This can be explained by the relaxation of the frameworks and the fact that the sites near the ions with long waiting time cannot be found in an early time region at low temperature. This tendency is remarkable for the low alkali content glass where the ionic motion is more coupled with the motion of the framework compared with high alkali content glasses. We found 159 sites for 144 Li ions for Li_2SiO_3

at 700 K during 4 ns run (Run II) and 210 sites for 192 Li ions for Li_4SiO_4 sites at 700 K during 2 ns run. These numbers obtained by the run up to diffusion regimes are about 10% larger than those of ions. The number for Li_2SiO_3 is larger than that obtained by Lammert *et al.* (3%) This may be due to the fact that they have excluded small clusters (corresponds to 7.6% of the number of ions) with small effective radius, which were explained as a satellite of the larger cluster and those in a saddlelike states of the small number. In our analysis, the latter is not included; however, the corresponding sites of the former are not excluded, because the small effective radius does not necessarily mean the small contribution to the dynamics. If we consider the differences mentioned above, the number of the sites determined for Li_2SiO_3 in this work is consistent to the analysis by them.

In our analysis, the sites are clearly separated from the saddle and the concept of the cluster or satellite seems to be meaningless. In a Li_4SiO_4 composition, still empty sites for jumps are found to be available. Larger number of sites was observed for the low alkali content glass with smaller diffusion coefficient. Thus the diffusion coefficient does not directly depend on the number of available jump sites and the concept of the cooperativity is necessary to explain the ion dynamics.

D. Sites for type A and B ions

The number of the sites for Li ions of A type and that for B type during 1 ns run (Run II of Li_2SiO_3 at 700 K in Table I) were counted. The number for type A ions is 146, while that of B sites is 98, and total number is 159. In this case, the number for type A and B ions is, 89 and 55, respectively. The number of sites characteristics for type A ions, those for type B ions and common sites are 61, 13, and 85, respectively. Thus we found many common sites for both types of ions. Many sites for type A ions are unchanged during the run because of long residence time, while type B sites characteristics to type B ions are forming conducting paths. Existence of the common sites suggests us that the difference of type A and B does not depend on the location in a fixed landscape. Results of detailed analyses for the small differences between the energy distributions of type A and B ions will be shown elsewhere.

E. Site energy distribution of type A and B ions

The energy distribution for type A and B in Run III at the beginning of the run is examined by the steepest descent method[17] and is shown in Fig. 5. The area under the distribution curve is normalized to 1 in each type. Most of lithium ions are located near the local minimum of the potential surface at every instance in the glassy state. The energy for each lithium ion includes, repulsive term, Ewald summation of Coulombic terms by all surrounding particles. As shown in this figure, site energy distribution for type A and B ions are almost the same in spite of the different character of the dynamics. Therefore, characteristics of the fast and slow dynamics are not based on the energy difference of the sites. It is necessary to consider the dynamics on the multidimensional potential surface including the motion of surrounding Li ions since structural difference between type A and B is dominant in an intermediate length scale as shown in the following section.

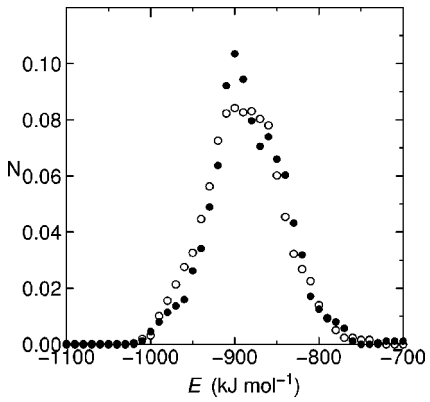

FIG. 5. Distributions of energies of type A and B of Li ions determined by the steepest descent method for Li_2SiO_3 at 700 K. The distributions have been normalized such that the area under each curve is 1. ○:type A, ●: type B ions.

F. Difference of structures for type A and B ions in the intermediate length scale

Microsegregation of the network modifier is evident from MD structure as well as from the empirically determined local structure[26] for ion conducting glasses. To learn the relationship between a density fluctuation in the microsegregated region and the diffusive dynamics, structural differences of type A and B ions were examined for both Li_2SiO_3 and Li_4SiO_4 glasses using the pair correlation functions $g(r)s$ with distinguishing types of ions. The $g(r)s$ during 1 ns run are shown here, since this time scale is suitable to distinguish type A and B ions clearly.

As shown in Fig. 6(a), pair-correlation functions $g(r)s$ of A-O and B-O pairs are essentially identical. Remarkable differences were found in the heights of the first and the second peaks, in $g(r)s$ of Li-Li pairs [Fig. 6(b)]. Higher peaks in B-B pair than in A-A pair mean that the type B ions are more densely packed, while smaller peak height of the third peak for B-B pair than A-A pair means that larger number of empty site is available for type B ions in the third coordination shell. The structure related to type B ion seems to be suitable to jump with neighboring ions of the same kind in cooperative manner. Such characteristics of the structure marked at arbitrarily chosen initial time are expected to be lost when the time scale of observation is much longer than the exchange rate of the slow and fast dynamics. These findings suggest us that structures in the intermediate length scale connecting the ion sites are essential to determine the characteristics of the ion dynamics, that is, the criteria of type A and B ions do not directly correspond to the property of energy of each site, instead, it depends on the geometrical arrangement of ion sites and ions considerably. As shown in Fig. 6(c), the peak height for B-B pair are larger than A-A pair not only for the first and second peaks but also for the third peak in Li_4SiO_4. Thus the cooperative motion of type B

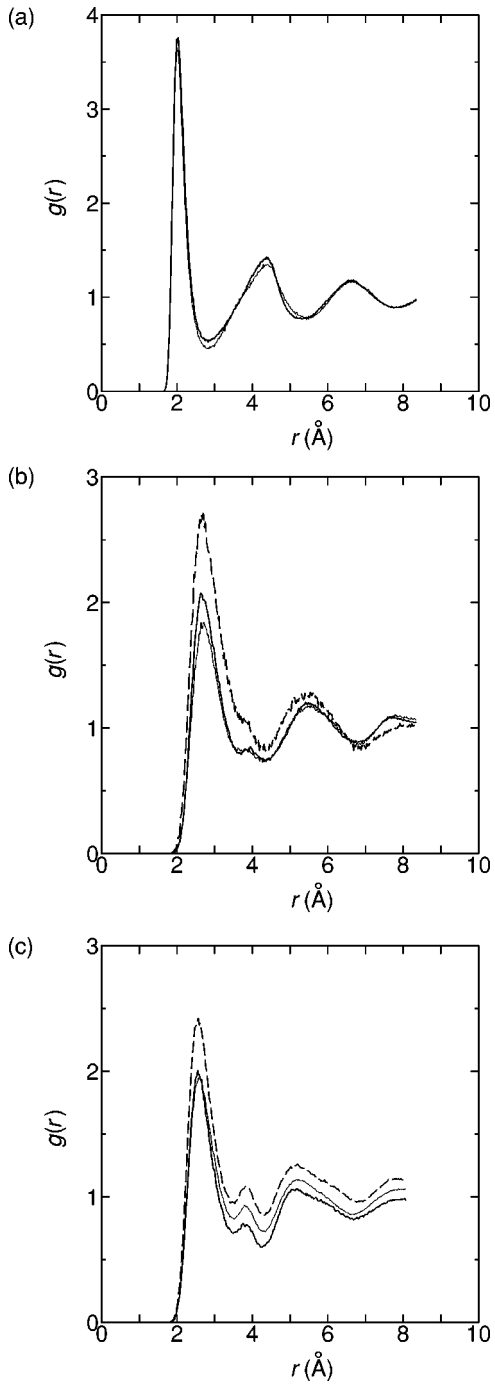

FIG. 6. Pair distribution functions $g(r)s$ with distinguishing type A and B ions for (a) A-O and B-O pairs for Li_2SiO_3 (b) A-A, B-B and A-B pairs for Li_2SiO_3 B-B and (c) A-A, B-B and A-B pair for Li_4SiO_4. Thick curve: A-O; thin curve: B-O in (a), thick curve: A-A, broken curve:B-B, thin curve: A-B in (b) and (c).

ions in this composition can include larger number of Li ions than in Li_2SiO_3. This result is consistent to the findings in Fig. 2(b), where the larger effective length scale of the jumps is observed. Differences in the pair correlation function, $g(r)$, for the Si-Li pair were also found when we distinguish the type A and B ions.

Recently, Varsamis *et al.*[27] have investigated the dynamic properties of Li ions in $0.3Li_2O$-$0.7B_2O_3$ glass by MD. When they have distinguished Li_b (reside predominantly in sites formed by bridging oxygen atoms) and Li_{nb} (sites involve both bridging and nonbridging oxygen atoms), it is found that the Li_{nb} is more mobile than Li_b type. There findings are consistent to ours because the Li_{nb} is surrounded by larger number of like ions than Li_b is.

Thus dynamics of Li ions in silicate glasses are linked to the microsegregation of the network modifier. Simultaneous jumps of neighboring ions in such structures make a large contribution to the diffusive dynamics. Although attention in this work is focused on the ion sites, activation energy for the jump motion play important roles to determine the dynamics. In Ref. 7, it was shown that a barrier height for the second lithium ion can be much lower than the first one when the cooperative jumps of two lithium ions occur, that is, the landscape is not fixed but is dynamical because the barrier height is strongly affected by the cooperative motion of the surrounding particles. Existence of the large ''mixed alkali effect,'' in the dilute foreign alkali region can be explained by the large ''cooperative blockage,'' where immobilization of one ion causes immobilization of other ions.[10] These facts suggest that the simple description by mobile vacancy is not adequate to characterize the ion dynamics. We would like to point out that the diffusive jumps of ions are not only sequential but also cooperative, where several ions jumps almost at the same time, and such jumps tend to repeat several times.[2,3] The motion is also affected by the coupling with surrounding atoms. Haven ratio, which is related to the ratio of the tracer diffusion and bulk diffusion (cross-correlation term), is one of the measures of the cooperativity. In some cases, contribution of this term may be neglected because the value is around 0.5 and the correction by this term is small. However, it should be noted that the strong forward correlation caused by the cooperative jumps is found in the single particle motion (tracer diffusion) and the Haven ratio is related to the further enhancement of this effect in the conductivity. Hence the importance of cooperativity in the ion dynamics should not be forgotten.

IV. CONCLUSION

We have investigated some characteristics of the potential energy surface to understand the mechanism of the ion conduction in glasses by using MD simulations. The method to count the available sites without using a cutoff value has been proposed and sites have been visualized by contour maps. The number of available sites in the Li_2SiO_3 system obtained within 4 ns run at 700 K is about 10% larger than the number of the ions. The numbers of sites in Li_4SiO_4 are not so different from that in Li_2SiO_3, while the diffusion coefficient of Li ion in Li_4SiO_4 is larger than Li_2SiO_3. This trend can be explained by the increased contribution of the fast dynamics by the cooperative jumps. We have compared the available sites for both slow (type A) and fast (type B) ions and found that there are common sites for type A and B ions besides the characteristic sites for each type of ions. On

the other hands, distributions of site energies of type A and B ions are quite similar. From the pair correlation functions with distinguishing type A and B ions, the density fluctuation of the Li ions in the intermediate length scale are found to be important to determine the difference between slow and fast dynamics. The role of cooperative jumps should be taken into account to understand the mechanism of the ion conduction of the glasses.

ACKNOWLEDGMENTS

One of the authors (J.H.) would like to thank K. Ngai, P. Maass, and A. Heuer for helpful discussions.

*Electronic address: jhabasak@n.cc.titech.ac.jp

[1] J. Habasaki, I. Okada, and Y. Hiwatari, Phys. Rev. E **52**, 2681 (1995).
[2] J. Habasaki, I. Okada, and Y. Hiwatari, Phys. Rev. B **55**, 6309 (1997).
[3] J. Habasaki and Y. Hiwatari, Phys. Rev. E **59**, 6962 (1999).
[4] A. Cormack, J. Du, and T. Zeitler, Phys. Chem. Chem. Phys. **4**, 3193 (2002).
[5] H. Lammert, M. Kunow, and A. Heuer, Phys. Rev. Lett. **90**, 215901 (2003).
[6] J. Habasaki and Y. Hiwatari, Phys. Rev. E **62**, 8790 (2000).
[7] J. Habasaki, I. Okada, and Y. Hiwatari, J. Non-Cryst. Solids **208**, 181 (1996).
[8] J. Habasaki, I. Okada, and Y. Hiwatari, J. Non-Cryst. Solids **183**, 12 (1995).
[9] J. Habasaki, I. Okada, and Y. Hiwatari, J. Phys. Soc. Jpn. **67**, 2012 (1998).
[10] J. Habasaki, K. L. Ngai, and Y. Hiwatari, J. Chem. Phys. (to be published).
[11] J.O. Isard, J. Non-Cryst. Solids **1**, 235 (1969).
[12] D.E. Day, J. Non-Cryst. Solids **21**, 343 (1976).
[13] M.D. Ingram, Phys. Chem. Glasses **28**, 215 (1987).
[14] M.D. Ingram, Glass Sci. Technol. (Frankfurt/Main, Ger.) **67**, 151 (1994).
[15] A. Khorassani and A.R. West, Solid State Ionics **7**, 1 (1982).
[16] J. Habasaki, K.L. Ngai, and Y. Hiwatari, Phys. Rev. E **66**, 021205 (2002).
[17] F. Stillinger and T.A. Weber, Phys. Rev. A **25**, 978 (1982).
[18] Y. Ida, Phys. Earth Planet. Inter. **13**, 97 (1976).
[19] J. Habasaki and I. Okada, Mol. Simul. **9**, 319 (1992).
[20] J. Habasaki and Y. Hiwatari, Phys. Rev. E **65**, 021604 (2002).
[21] M.F. Shlesinger, G.M. Zaslavsky, and J. Klafter, Nature (London) **363**, 31 (1993).
[22] J. Klafter, M.F. Shlesinger, and G. Zumofen, Phys. Today **49**, 33 (1996).
[23] S. Alexander and R. Orbach, J. Phys. (Paris), Lett. **43**, L625 (1982).
[24] P. Maass, J. Non-Cryst. Solids **255**, 35 (1999).
[25] J. Habasaki, Y. Hiwatari, and I. Okada, Mater. Res. Soc. Symp. Proc. **455**, 91 (1997).
[26] G.N. Greaves, Y. Vaills, S. Sen, and R. Winter, J. Optoelectron. Adv. Mater. **2**, 299 (2000).
[27] C.P.E. Varsamis, A. Vegiri, and E.I. Kamitsos, J. Non-Cryst. Solids **307**, 956 (2002).